Crystallization and Photovoltaic Properties of Titania-Coated Polystyrene Hybrid Microspheres and Their Photocatalytic Activity

Ming Zhang, Ge Gao, Dacheng Zhao, Zhiying Li, and Fengqi Liu*

College of Chemistry, Jilin University, Changchun 130023, P.R. China

Received: December 25, 2004; In Final Form: March 14, 2005

The hybrid microspheres with polystyrene core coated by titania nanoparticles were prepared by miniemulsion polymerization, and the as-prepared samples were characterized by SEM, XRD, TG-DTA, XPS, and SPS techniques. TiO_2 nanoparticles experienced two processes of phase transition, i.e., amorphous to anatase and anatase to rutile at the calcining temperature range from 400 to 1000 °C. The phase transformation temperature of TiO_2 hybrid microspheres from anatase to rutile was increased by about 300 °C due to the blocking function of calcined polymer remainder. SPS results present that the band-gap of hybrid microspheres is 3.2−3.4 eV, which is larger than that of pure TiO_2. The maximum intensity of the SPS signal is about 3 times larger for the hybrid material as compared to the pure TiO_2. In addition, the photocatalytic degradation rate of TiO_2 hybrid microspheres was 15% faster than that of pure TiO_2 in the experiment of the photocatalytic degradation of methyl orange.

1. Introduction

Titanium dioxide is, to date, not only the most important synthetic pigment, but also, due to its outstanding electronic properties, one of the most photoactive catalysts, and because of its high chemical stability and nontoxicity, one of the most practical materials employed in heterogeneous photocatalysis.[1] Extensive research has been carried out to explore its widespread applications such as degradation of hazardous volatile organic and malodorous compound, decolorization of dyeing wastewater, direct decomposition of NO_x and SO_x, and purification of air and water.[2−4] The catalytic properties of titania depend on its crystal modification and crystallinity, and can be further tuned by doping and by structuring.[5] Furthermore, the catalytic activity of TiO_2 also depends strongly on electron−hole separation, and the key of the photocatalytic process is to inhibit the recombination of electron and hole.[6]

It is well-known that it is the anatase polymorph rather than the brookite or rutile polymorphs that has the highest photocatalytic activity. The difficulty in producing an extremely active, phase-pure anatase photocatalyst stems from the fact that rutile is the thermodynamically stable polymorph, and although anatase is kinetically stable, it is readily converted to the rutile phase in the temperature range of 600−1000 °C.[7] Therefore it is desirable to find a way to enhance the phase transition temperature from anatase to rutile and to extend the temperature range in which the anatase phase is stable.

Crystallization property and phase transformation in titania have been widely studied from the point of view of both scientific interest and technological applications.[1,8] It has also been found that there exists a significant particle-size effect on the transformation rate for nanocrystalline TiO_2. Furthermore, the photocatalytic activity can be increased dramatically with the decrease of the particle size of photocatalyst.[9,10]

In previous work[11] we have prepared hybrid microspheres with a polystyrene core coated by titania nanoparticles by miniemulsion polymerization for the first time and characterized their morphologies. Our present work focuses mainly on the morphology, crystallization, and surface photovoltage properties and photocatalytic activity by using scanning electron microscope (SEM), XRD, thermogravimetry-differential thermal analysis (TG-DTA), X-ray photoelectron spectrometer (XPS), and surface photovoltage spectra (SPS). The transition temperature from anatase to rutile of TiO_2 hybrid microspheres prepared by the method was increased. The results show that the nanocomposite exhibits good features, such as heat-stability and wide band-gap, indicating that it is a promising prospect in photocatalysis.

2. Experimental Section

The detailed preparation method of TiO_2 coated polystyrene hybrid microspheres was published in our previous work.[11] The recipe is as follows: 20 mL of deionized water, 0.01 g of the surfactant cetyltrimethylammonium bromide (CTAB), 5 g of TiO_2 colloid, 0.05 g of azobisisobutyronitrile (AIBN), 0.05 g of hydrophobic agent, 1 mL of styrene, and 0.2 mL of acrylic acid. All the chemicals were added in the above order with continued stirring (120 rpm). The reaction was conducted at 60 °C for 12 h.

Sample A is pure TiO_2 prepared by sol−gel, and sample B is TiO_2 coated polystyrene hybrid microsphere. Sample C was prepared with the following method, in which 0.5 mL of acrylic acid and 0.025 g of AIBN were added to B latex, followed by polymerization at 60 °C for 8−10 h. After being dried under decompression, samples were heated to different temperatures at a rate of 1 deg C/min, and kept at the desirable temperature for 2 h.

The morphologies of TiO_2 coated polystyrene spheres were characterized with a SHIMADZU SSX-550 scanning electron microscope. The crystallization structure of samples was characterized with a Rigaku wide-angle X-ray diffractometer (D/max γA, using Cu Kα radiation at wavelength $\lambda = 1.541$ Å). The detector was calibrated by using KCl powders as standard with 2θ being 28.345° (200) and 40.507° (220) under Cu Kα radiation. The thermal properties were measured with a

10.1021/jp044122f CCC: $30.25
Published on Web 04/12/2005

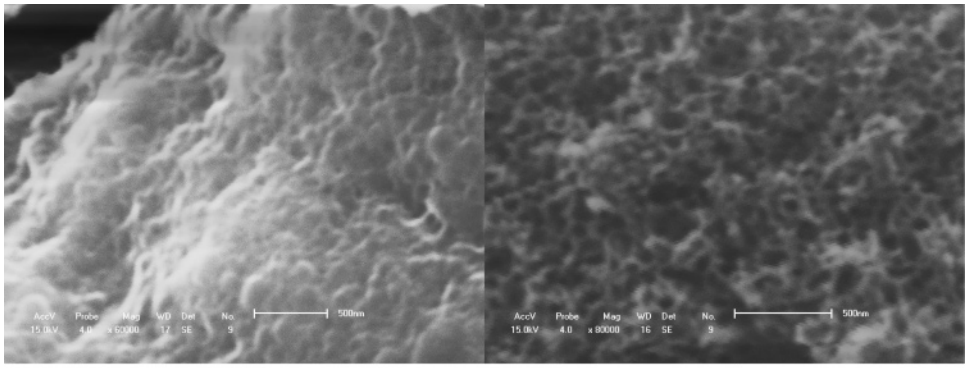

a b

Figure 1. SEM photographs of sample B (a) dried at room temperature and (b) calcined at 600 °C.

NETZSCH STA 449C TG-DTA. X-ray photoelectron spectroscopy measurements were performed with a VG ESCALAB MKII. The SPS measurements of the samples were carried out with a home-built apparatus that has been described elsewhere.[12,13]

Sample A or B (0.05 g) calcinated at 600 °C was added to methyl orange solution, then the catalyst powder was suspended in solution by ultrasonics. The solution was irradiated with a 8 W ultraviolet lamp and sampled at a given time. Samples were analyzed with a spectrophotometer after TiO_2 powder was removed by centrifugation.

3. Results and Discussion

3.1. The Morphologies of Coated Microspheres. Figure 1, parts a and b, shows SEM photographs of TiO_2-coated polystyrene particles dried at room temperature or calcinated at 600 °C (sample B), respectively. During drying, free TiO_2 congregated around hybrid particles functioning as a filler. After the sample was calcinated at 600 °C, polymer was burned out and the sample presented microporus morphology with a 50 nm aperture. The microporus structure enables the sample to have larger adsorbent capacity.

3.2. Crystallization Behavior of TiO_2. Parts a−c of Figure 2 show XRD photographs of samples A, B, and C calcinated at different temperatures. The average crystallite size and the weight percentage of the anatase phase of TiO_2 nanoparticles calcined at different temperatures were calculated (shown in Table 1). Figure 2a displays that the TiO_2 nanoparticles presented anatase structure below 500 °C, formed rutile crystallization in the range of 500−800 °C, and transited totally into rutile above 800 °C, which is consistent with other author's reports.[9,14] However, hybrid sample B only formed 17% rutile crystallization at 800 °C, and showed all anatase phase below 800 °C, which means that the transition temperature from anatase to rutile was increased by about 300 °C by hybridization with polymers. Although polymer in the core−shell microspheres was burnt below 400 °C, the remaining polymer still played a role in obstructing TiO_2 by arraying further and forming rutile crystallization. Even though most of the polymer in shell-core microspheres was burnt out above 600 °C, there still remained some, whose blocking function made the crystallization of titania in hybrid particles not perfect. In the meantime the burning rate of polymer was faster than that of shrinking resulting from crystallization of titania, leaving vacancies occupied originally by polymer particles and preventing the transition of titania from anatase to rutile. From the data listed in Table 1 we can determine that the crystallite sizes of hybrid samples B and C at different temperatures were all smaller than that of the nonhybrid sample, which also provided further evidence for the above phenomenon. When temperature was increased further, the crystallite sizes of titania were continually enlarged until all rutile crystallization was finally formed at 900 °C.

TABLE 1: XRD and SPS Data

sample	calcinting temp (°C)	anatase content (%)	crystallite size of anatase (nm)	surface photovoltage (mV)	threshold (eV)
A	400	100	7.768		
	500	67.75	11.66	0.229	3.258
	600	47.15	17.55	0.136	3.134
	700	40.12	30.10	0.141	3.053
	800	0		0.0199	3.048
B	400	100	4.56		
	500	100	7.17	0.0131	3.381
	600	100	13.99	0.226	3.366
	700	100	20.85	0.476	3.317
	800	88.45	28.82	0.796	3.311
	900	0		0.0131	3.112
	1000	0			
C	400	100	4.84		
	500	100	5.145	0.318	3.417
	600	100	6.588	0.231	3.404
	700	100	8.74	0.139	3.408
	800	54.78	10.3	0.0341	3.142
	900	9.52	35.59		
	1000	0			

The crystallite sizes of samples A and B became larger as the temperature increased, and the crystallite sizes of samples A and B were about the same, with only sample C being quite different (Figure 3). Similarly, the crystallite size of sample C increased with the temperature; however, the size increase was not as dramatic as with samples A and B. The difference resulted from the fact that for sample C the amount of free TiO_2 particles was reduced when more acrylic acid was added.

3.3. Thermal Properties. The unordinary crystallization phenomenon of hybrid samples may get support from the results of TG (Figure 4). The weight losses of sample B stood at about 10% (only being polymer weight and not including TiO_2) below 340 °C and about 32% in the range of 340−430 °C, and the average thermogravimetric rate was 0.36%/deg. The thermogravimetric rate slowed above this temperature range and tended to be constant at about 650 °C. Even calcinated at 800 °C, the sample left about 40% polymer, which functioned to prevent the transition of titania from anatase to rutile.

3.4. XPS Results. The results of TG showed that the weight of the remaining sample was 39.36% (mass %) when it was calcinated at 650 °C. The mass percent of titania calculated according to the recipe is about 20%, implying that some polymers were graphitized for not being burnt out completely. The results of XPS strongly support this postulate. Figure 5

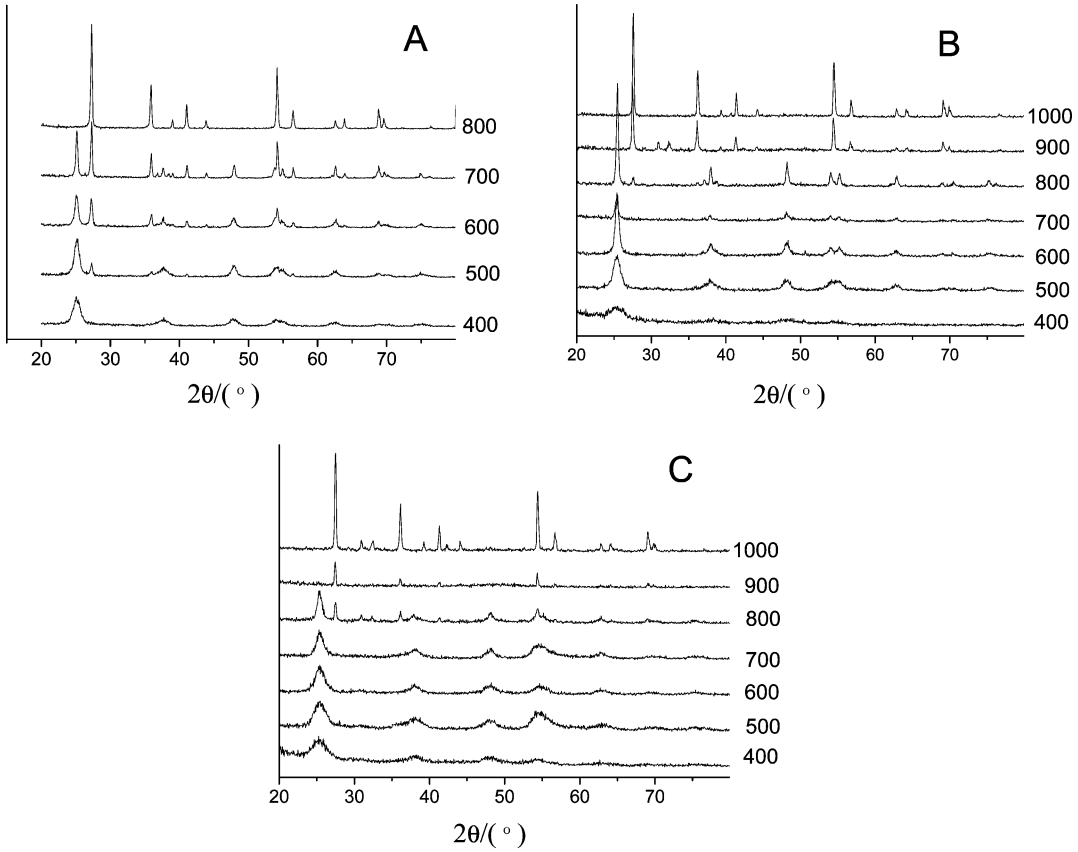

Figure 2. XRD diagrams of samples calcined at different temperatures: (A) sample A; (B) sample B; (C) sample C.

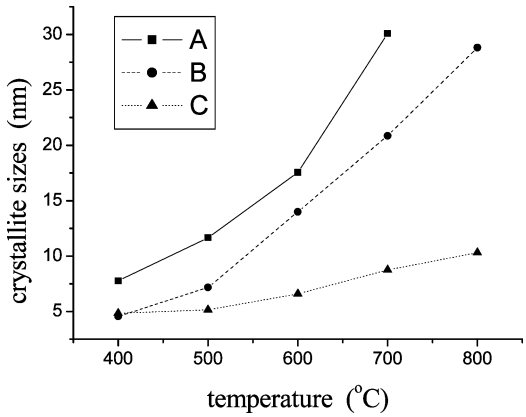

Figure 3. Change of crystallite sizes with temperature: (A) sample A; (B) sample B; (C) sample C.

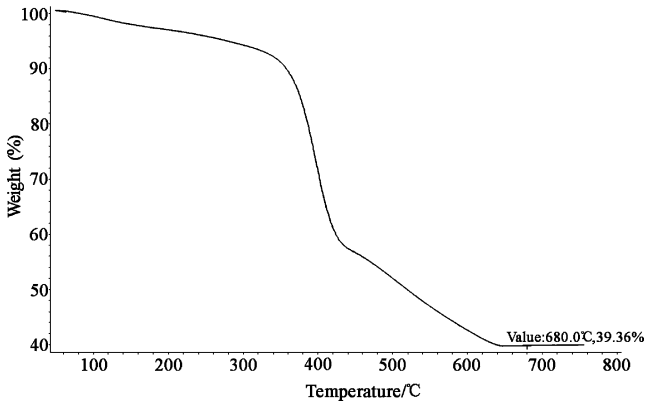

Figure 4. TG curve of sample B.

displays XPS diagrams of samples A and B calcinated at 600 or 800 °C. The measured binding energy of C_{1s} in hybrid particles is 283.8 eV, that of adsorption carbon is 284.6 eV, and that of C_{1s} in graphite is 284.2 eV according to the standard diagram, so carbon in hybrid particles has been graphitized. There only existed peaks of Ti−O and H−O bonds from the O spectrum, meaning that C−O bonds were fully fractured during the calcination and hydroxys were adsorbed onto the surface of hybrid microspheres. From the peak area we can calculate the mass percentage of Ti, C, and O respectively, C 28.76% and hydroxy 3.47% at 600 °C, and C 26.28% and hydroxy 6.49% at 800 °C, and there existed only Ti, C, and O elements at 800 °C. However, graphitized carbon in the remainder (39.36%) amounts to 10.34% and the percentage of TiO_2 should be 29.02%. Comparing the remaining TiO_2 with that in the recipe, we learn that the percentage of TiO_2 is a little high. One explanation for this phenomenon is that the XPS technique only detects 3−5 nm of depth in samples and some carbons were coated in the shell of TiO_2. Anther reason results from the fact that the conversion rate in synthesis is not as high as 100%. By calculating we knew that the ratio of Ti to O is 1:2, and the binding energy of Ti is 458.8 eV, which is consistent with that of Ti_{2p}^{4+} according to the data provided from the standard database, indicating that Ti exists in the Ti^{4+} form on the surface of hybrid particles and the chemisorbed oxygen is the contribution of the surface hydroxyl.

3.5. SPS of TiO_2. The photocatalytic activity of TiO_2 depends strongly on the separation of electron and hole. The key in photocatalytic process is to inhibit the recombination of electron with the hole.[7] The catalytic properties of material can be predicted by using SPS to measure its photoelectricity. Parts a and b of Figure 6 reveal the SPS of samples A and B calcined at different temperatures. We can see that for all the samples there is a broad absorption band from 300 to 400 nm that is due to the transition of the O^{2-} antibonding orbital to the lowest

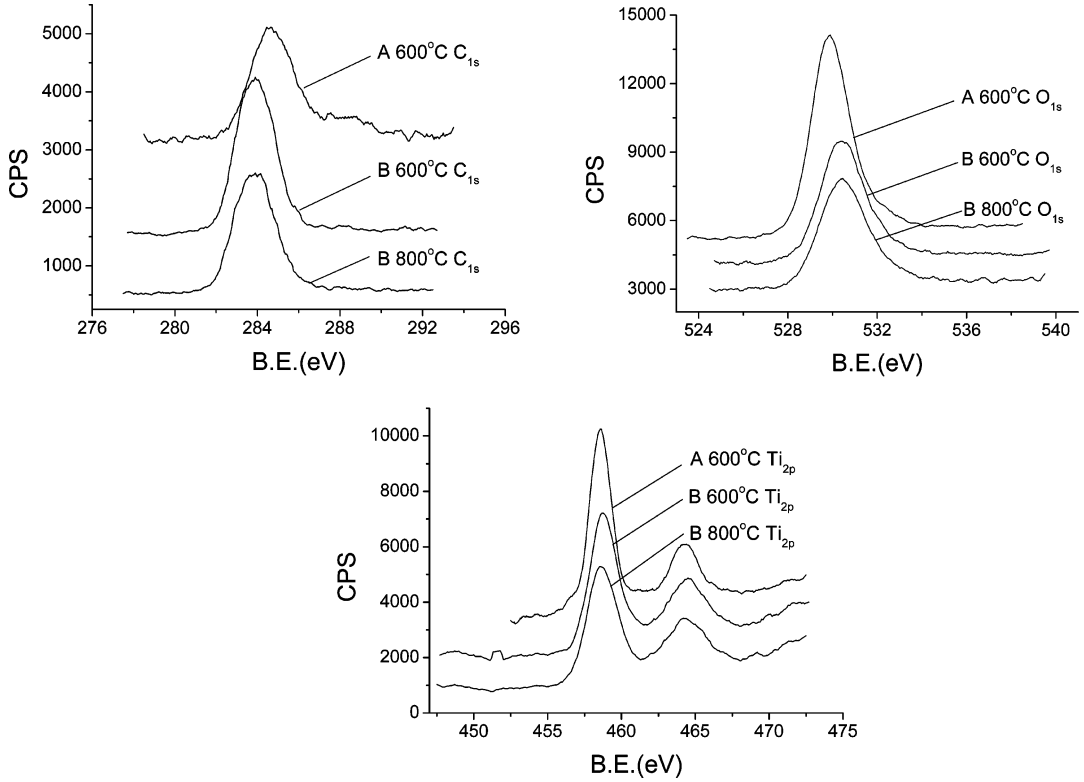

Figure 5. XPS photographs of samples A and B calcined at 600 or 800 °C.

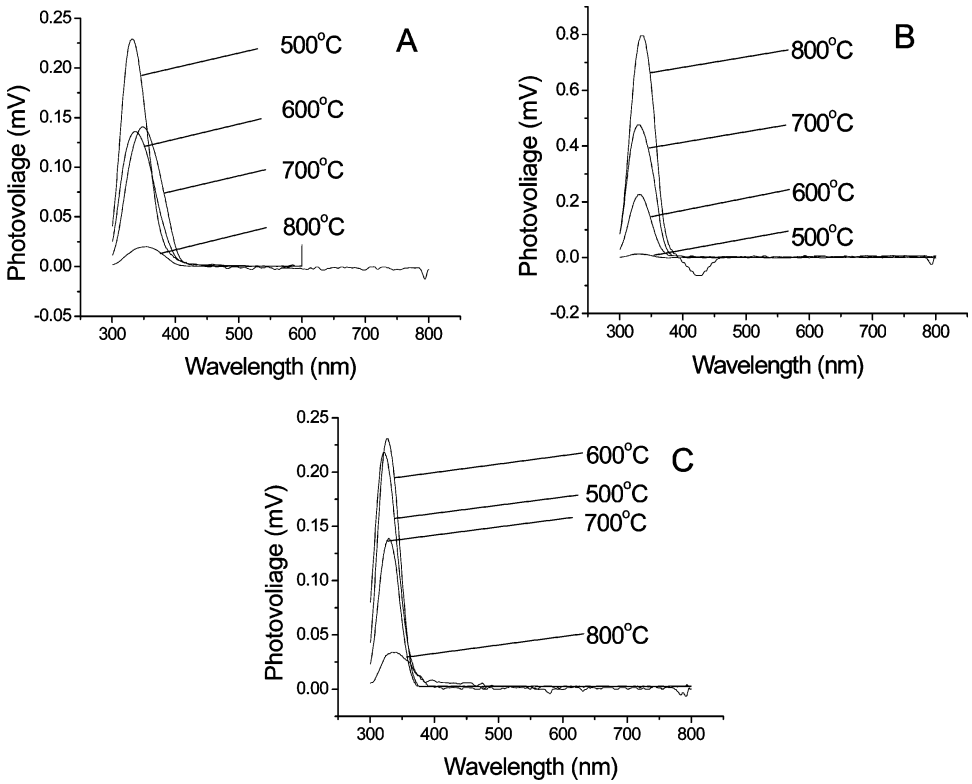

Figure 6. SPS photographs of samples at different calcination temperatures: (A) sample A; (B) sample B; (C) sample C.

empty orbital of Ti^{4+} and the blue shift of the optical edge is attributed to the quantum size effect.

The threshold values of samples A and B decrease with the increase in temperature (see Table 1), and the threshold value of sample B is always higher than that of sample A. It is commonly known that the crystallization morphology of titania plays a critical role in determining the magnitude of the threshold value.[15,16] Generally, the threshold value of anatase TiO_2 is higher than that of rutile TiO_2. For the same crystal form due to the quantum size effect the smaller its crystallite is, the bigger its threshold value is.[17−19]

The phase transformations of TiO_2 nanoparticles from anatase to rutiles occurred with the increase of calcination temperature. So its threshold value became small. However, sample B presented anatase below 800 °C because of the blocking function of polymers. The increase of the threshold value and the

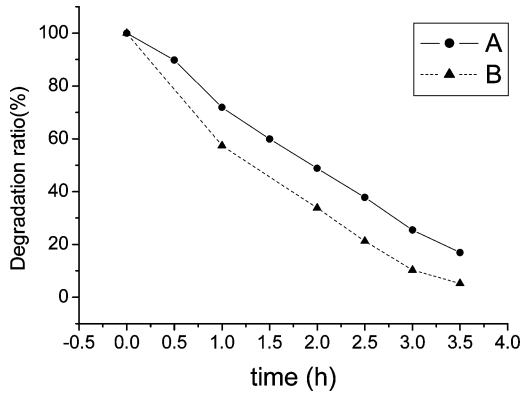

Figure 7. The relationship of degradation ratio with time: (A) sample A and (B) sample B.

widening of the band-gap resulted in the enhancement of the redox capability of the photoelectron and the hole, which improves the efficiency of photodegradation. It can be predicted that the photodegradation activity of hybrid particles should be higher than that of pure TiO_2 nanoparticles by comparing their threshold values.

The threshold values of sample B was smaller than that of sample C, in which the addition of more acrylic acid decreased the amount of free TiO_2 particles and induced the particle size to become small, thus having a higher threshold value due to the quantum size effect.

The maximum intensity of the SPS signal of sample B was three times as large as that of sample A, which would be attributed to the synergistic effects of doping graphitizing carbon in TiO_2, OH groups enriched on the surface of hybrid microspheres, and the quantum size effect, which promote the separation of electron and hole and induce the increase of surface photovoltage.

3.6. Catalytic Experiment. To examine the catalytic property a parallel test was conducted with pure TiO_2 and hybrid TiO_2 in methyl orange solution (see Figure 7). The photocatalytic degradation rate of sample B was 15% quicker than that of sample A with a 95% degradation ratio in 3.5 h, which proves the hybrid microspheres have better catalytic activity. According to Hoffmann's explanation if a surface defect state is available to trap the electron or hole, recombination is prevented and subsequent redox reactions may occur.[20] The residue of polymer left after calcination blocked crystallite growth and made the crystal surface imperfect, so the photocatalytic activity was enhanced.

4. Conclusions

Polymers in hybrid microspheres have an effect on crystallization and surface photovoltaic properties of TiO_2. The transition temperature of hybrid microspheres from anatase to rutile is increased to the range of 800−1000 °C. SPS results present that the band-gap of hybrid microspheres is 3.2−3.4 eV, which is larger than that of pure TiO_2. The maximum intensity of the SPS signal is about 3 times larger for the hybrid material as compared to that of the pure TiO_2. In the experiment of photocatalytic degradation of methyl orange, the photocatalytic degradation rate of TiO_2 hybrid microspheres is 15% faster than that of pure TiO_2 prepared by our group, demonstrating that hybrid microspheres are superior to pure TiO_2 in photocatalytic activity. The work on the catalytic mechanism and structure of hybrid microspheres is under way.

Acknowledgment. We thank the National Natural Science Foundation of China (20274014) and the Chinese Ministry of Education through the teaching and research award fund for outstanding young teachers in higher education institutions for financial support.

References and Notes

(1) Zhang, Y.; Ebbinghaus, S. G.; Weidenkaff, A.; Kurz, T.; Krug von Nidda, H.-A.; Klar, P. J.; Güngerich, M.; Reller, A. *Chem. Mater.* **2003**, *15*, 4028.

(2) Shklover, V.; Nazeeruddin, M.-K.; Zakeeruddin, S. M.; Barbé, C.; Kay, A.; Haibach, T.; Steurer, W.; Hermann, R.; Nissen, H.-U.; Grätzel, M. *Chem. Mater*. **1997**, *9*, 430.

(3) Chen, D.-W.; Ray, A. K. *Appl. Catal. B* **1999**, *23*, 143.

(4) Jing, L.-Q.; Sun, X.-J.; Cai, W.-M.; Xu, Z.-L.; Du, Y.-G.; Fu, H.-G. *J. Phys. Chem. Solids* **2003**, *64*, 615.

(5) Litter, M. I.; Navío, J. A. *J. Photochem. Photobiol. A* **1996**, *98*, 171.

(6) Fujishima, A.; Rao, T. N.; Tryk, D. A. *J. Photochem. Photobiol. C* **2000**, *1*, 1.

(7) Yanagisawa, K.; Ovenstone, J. *J. Phys. Chem. B* **1999**, *103*, 7781.

(8) Hu, Y.; Tsai, H.-L.; Huang, C.-L. *Mater. Sci. Eng. A* **2003**, *344*, 209.

(9) Xu, Z.-L.; Shang, J.; Liu, C.-M.; Kang, C.-L.; Guo, H.-C.; Du, Y.-G. *Mater. Sci. Eng. B* **1999**, *56*, 211.

(10) Zhang, Q.; Gao, L.; Guo, J. *Appl. Catal. B* **2000**, *26*, 207.

(11) Zhang, M.; Gao, G.; Li, C.; Liu, F. *Langmuir* **2004**, *20*, 1420.

(12) Xie, T. F.; Wang, D. J.; Chen, S. M.; Li, T. J. *Thin Solid Films* **1998**, *327*−*329*, 415.

(13) Du, H.; Cao, Y.; Bai, Y.; Zhang, P.; Qian, X.; Wang, D.; Li, T.; Tang, X. *J. Phys. Chem. B* **1998**, *102*, 2329.

(14) Kimura, I.; Kase, T.; Taguchi, Y.; Tanaka, M. *Mater. Res. Bull.* **2003**, *38*, 585.

(15) Shang, J.; Xu, Z. L.; Du, Y. G.; Li, J. M. *J. Inorg. Mater.* **2001**, *16*, 1211.

(16) Zhu, L.; Wang, D. J.; Xie, T. F.; Shang, J.; Xu, Z. L.; Du, Y. G. *Chem. J. Chin. Univ.* **2001**, *22*, 827.

(17) Brus, L. *J. Phys. Chem.* **1986**, *90*, 2555.

(18) Jing, L.; Sun, X.; Shang, J.; Cai, W.; Xu, Z.; Du, Y.; Fu, H. *Sol. Energy Mater. Sol. Cells* **2003**, *79*, 133.

(19) Steigerwald, M. L.; Brus, L. E. *Acc. Chem. Res.* **1990**, *23*, 183.

(20) Hoffmann, M. R.; Martin, S. T.; Choi, W.; Bahnemann, D. W. *Chem. Rev.* **1995**, *95*, 69.